

10.24425/acs.2020.132586

Archives of Control Sciences
Volume 30(LXVI), 2020
No. 1, pages 77–100

Global path planning for multiple AUVs using GWO

MADHUSMITA PANDA, BIKRAMADITYA DAS and BIBHUTI BHUSAN PATI

In global path planning (GPP), an autonomous underwater vehicle (AUV) tracks a pre-defined path. The main objective of GPP is to generate a collision free sub-optimal path with minimum path cost. The path is defined as a set of segments, passing through selected nodes known as waypoints. For smooth planar motion, the path cost is a function of the path length, the threat cost and the cost of diving. Path length is the total distance travelled from start to end point, threat cost is the penalty of collision with the obstacle and cost of diving is the energy expense for diving deeper in ocean. This paper addresses the GPP problem for multiple AUVs in formation. Here, Grey Wolf Optimization (GWO) algorithm is used to find the suboptimal path for multiple AUVs in formation. The results obtained are compared to the results of applying Genetic Algorithm (GA) to the same problem. GA concept is simple to understand, easy to implement and supports multi-objective optimization. It is robust to local minima and have wide applications in various fields of science, engineering and commerce. Hence, GA is used for this comparative study. The performance analysis is based on computational time, length of the path generated and the total path cost. The resultant path obtained using GWO is found to be better than GA in terms of path cost and processing time. Thus, GWO is used as the GPP algorithm for three AUVs in formation. The formation follows leader-follower topography. A sliding mode controller (SMC) is developed to minimize the tracking error based on local information while maintaining formation, as mild communication exists. The stability of the sliding surface is verified by Lyapunov stability analysis. With proper path planning, the path cost can be minimized as AUVs can reach their target in less time with less energy expenses. Thus, lower path cost leads to less expensive underwater missions.

Key words: Autonomous Underwater Vehicle (AUV), Genetic Algorithm(GA), Global Path Planning (GPP), Grey Wolf Optimization(GWO), Sliding Mode Control (SMC), waypoints

1. Introduction

In recent time, AUVs are employed in commercial mission along with scientific research and military missions. Underwater mission planning with multiple

Copyright © 2020. The Author(s). This is an open-access article distributed under the terms of the Creative Commons Attribution-NonCommercial-NoDerivatives License (CC BY-NC-ND 3.0 <https://creativecommons.org/licenses/by-nc-nd/3.0/>), which permits use, distribution, and reproduction in any medium, provided that the article is properly cited, the use is non-commercial, and no modifications or adaptations are made

Madhusmita Panda and Bikramaditya Das are with Department of Electronics and Telecommunication, VSSUT, Burla, Odisha, India.

Bibhuti Bhusan Pati is with Department of Electrical Engineering, VSSUT, Burla, Odisha, India.

Received 2.6.2019. Revised 1.02.2020.

AUVs needs cooperative path planning to reduce time and energy costs. Hence, the battery powered AUVs can cover larger areas in less time. Cooperative path planning control is a difficult task to achieve due to the uncertainties in AUV dynamics and underwater environment [1]. Again, absence of global positioning system (GPS) signals increase the difficulty in communication in underwater environment [2]. Formation control with communication constraint employing “adaptive sliding mode control (adaptive SMC)” [3], “nonlinear observer” [4] and “neural network (NN)” [5] are advocated in literature. Majorities of these researches deal with formation control based on leader-follower architecture. Formation control of AUVs can be studied under two heads “regulatory control” and “tracking control” [6]. The former focuses on maintaining a specified shape of formation while the later tracks a specified path to reach the destination. A* algorithm for 3D path planning has been used to generate optimal paths in larger grid with static obstacles [7]. Evolutionary algorithms such as “genetic algorithm (GA)”, “memetic algorithm (MA)”, “particle swarm optimization (PSO)”, “ant colony optimization (ACO)” and “shuffled frog leaping algorithm (SFLA)” are suggested to generate time and energy efficient paths, by minimizing a nonlinear time-energy cost function [8, 9].

GA is an effective local search technique that can solve multi-objective optimization problem. GA concept is easy to understand and can implemented easily. It is also robust to local maxima and minima. Thus, it is preferred to solve multitude of problems related to science, engineering and commerce. Ataei et al. [10] proposed a 3D path planner employing GA to generate optimal trajectory for an AUV using “waypoint guidance”. The major challenge is to successfully navigate the AUV in a dynamic oceanic environment while avoiding collision with the obstacles. Modelling an objective function in GA and proper representation of genetic operators are quite difficult. GA requires longer processing time that increases the computational cost.

“Grey Wolf Optimization (GWO)” is recent meta-heuristic algorithm belongs to Swarm Intelligence (SI) methods. SIs are “population-based meta-heuristics” that imitate the nature of herds, flocks, swarms and schools of animal. GWO depicts the hunting procedure of Grey Wolves [11]. Grey wolves are pack hunters and follow hierarchical hunting pattern. GWO is different from other SI algorithm as it prevails the social hierarchy in hunting as found in grey wolf pack [12]. GWO provides high level of exploration and exploitation. It provides better approximation of the weighted path cost with less computationally expanses while avoiding local optima [11]. Various applications of GWO are surveyed in [13]. Using GWO we can explore all most all the benefits of GA with less computational cost. Hence, GWO can be used instead of GA for planning optimal path for AUV in 3D environment.

Generating optimal paths for unmanned aerial vehicle (UAV) has been very well studied in literature [14–16]. Radmanesh et al. [14] used GWO to find the

optimized path for an “unmanned aerial vehicle (UAV)” in presence of “intruder aircrafts (IAs)”. IAs are the moving obstacles with unpredictable trajectories. Yao et al. [15] solved 3D GPP problem in the presence of terrains by using a hybrid GWO algorithm. GPP in 2D environment employing GWO has been proposed by Zhang et.al [16] for the “unmanned combat aerial vehicle (UCAV)”. The simulation results show better quality and stability as compared to other algorithms such as “cuckoo search (CS)”, “flower pollination algorithm (FPA)” etc., employed for solving the same problem. The results obtained in the above mentioned researches inspired us to use GWO in finding an optimal path for multiple AUVs in formation under mild communication. In our previous works, we have applied GWO for global path planning of a single AUV [17] and also reviewed path planning algorithms used for AUV path planning [18]. But, GWO is yet not applied to address path planning issues of multiple AUVs in formation. The proposed method will increase the efficiency and longevity of any underwater mission involving multiple AUVs by saving the time and energy, and thus reduces the mission cost.

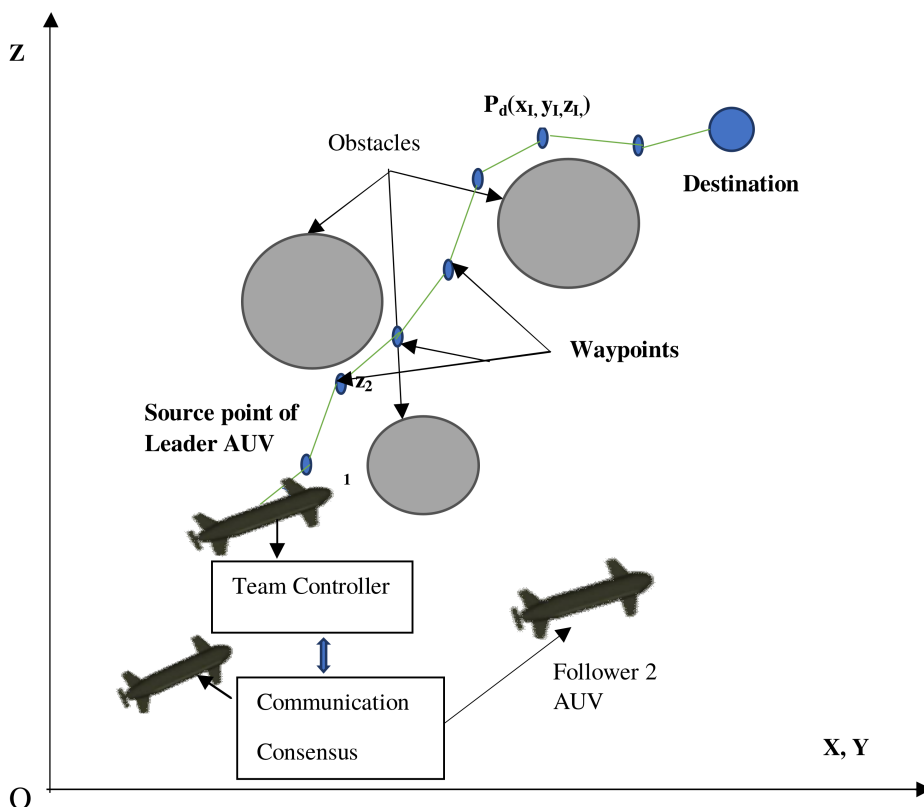


Figure 1: GPP scheme under communication constraints

The contributions of the paper can be briefed as follows:

- Applying GWO to generate a sub-optimal path for AUV.
- The performance of the proposed GWO path planner is compared with the well-known GA path planner results considering obstacle free, moderate obstacle and obstacle rich environment. The comparisons show GWO produces optimized cost path.
- Considering the better results obtained, GWO is used for planning optimal path for three AUVs in formation by a nonlinear SMC controller.

This research work further discusses the AUV dynamics and SMC controller in section 2, problem formulation in section 3, communication consensus in section 4, review of GWO and its application to GPP of AUV in section 5, result discussion in section 6 respectively and finally concludes in section 7.

2. Preliminaries

2.1. AUV dynamics

The continuous system can be represented as

$$\ddot{\lambda}_k = (\dot{\lambda}_k, \tau_k), \quad (1)$$

where $\lambda_k = [\lambda_1, \lambda_2]^T$ is the position and orientation vector of k -th AUV in inertial frame with $\lambda_1 = [x_k, y_k, z_k]^T$ and $\lambda_2 = [\phi_k, \theta_k, \psi_k]^T$. The control input Γ_k depended on both states generated by controller and state provided by team controller. AUV kinematic and dynamic for six-DOF, while the AUV is moving in 3D space is as shown in figure below [19].

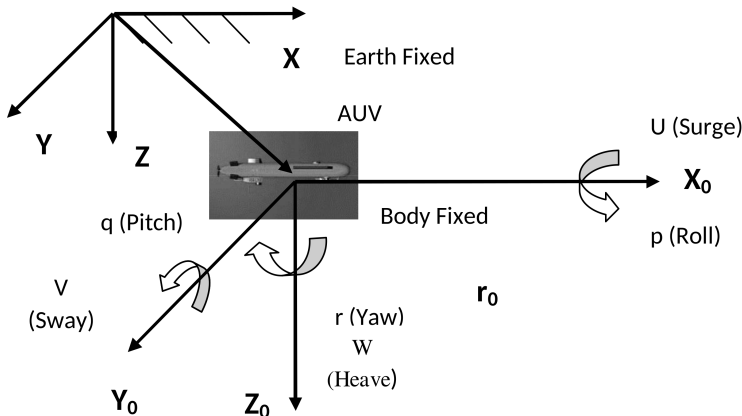


Figure 2: Body fixed and Earth fixed frame of reference for AUV [18]

The velocity matrix is defined as

$$V_k = [V_1, V]^T \quad \text{with } V_1 = [u_k, v_k, w_k]^T \quad \text{and } V_2 = [p_k, q_k, r_k]^T. \quad (2)$$

The defined 6 DOF dynamic equations of motion of an AUV is given by [20]

$$\mathfrak{M}\dot{V} + C(V)V + D(V)V + G(\lambda) = \Gamma. \quad (3)$$

The mass matrix \mathfrak{M} is defined as

$$\mathfrak{M} = \begin{bmatrix} \mathcal{M}_1 & 0 \\ 0 & \mathcal{M}_2 \end{bmatrix}, \quad (4)$$

where, the inertial mass matrix is $\mathcal{M}_1 = \begin{bmatrix} m_{11} & 0 & 0 \\ 0 & m_{22} & 0 \\ 0 & 0 & m_{33} \end{bmatrix}$ is and the added mass

matrix is $\mathcal{M}_2 = \begin{bmatrix} m_{44} & 0 & 0 \\ 0 & m_{55} & 0 \\ 0 & 0 & m_{66} \end{bmatrix}$.

The corolis and centripetal matrix is given as

$$C(V) = \begin{bmatrix} 0 & C(V_1) \\ C_1(V_1) & C_2(V_2) \end{bmatrix}. \quad (5)$$

The damping matrix defined as

$$D(V) = \begin{bmatrix} D_1(V_1) & 0 \\ 0 & D_2(V_2) \end{bmatrix}. \quad (6)$$

$G(\lambda)$ represents effect of gravitational and buoyancy forces, which depends on water density ρ , gravitational acceleration g , displaced volume ϑ , transverse metacentric height $\bar{G}\bar{M}_T$ longitudinal metacentric height $\bar{G}\bar{M}_L$, and is given by

$$G(\lambda) = \begin{bmatrix} 0 & 0 & 0 & \rho g \vartheta \bar{G}\bar{M}_T \sin(\psi) & \rho g \vartheta \bar{G}\bar{M}_L \sin(\psi) & 0 \end{bmatrix}^T. \quad (7)$$

Γ is the force and moments matrix, represented as

$$\Gamma = \begin{bmatrix} \Gamma_1 & \Gamma_2 \end{bmatrix}^T. \quad (8)$$

The 6-DOF mathematical model of an AUVs in “Earth Fixed Reference frame (EFR)” can be defined by using the kinematics equation $\dot{\lambda} = \mathfrak{R}(\lambda)v$ and $\ddot{\lambda} = \mathfrak{R}(\lambda)\dot{v} + v\mathfrak{R}(\lambda)$, as

$$\mathcal{M}_\lambda(\lambda)\ddot{\lambda} + C_\lambda(\dot{\lambda}, \lambda)\dot{\lambda} + D(\dot{\lambda}, \lambda)\dot{\lambda} + g_\lambda(\lambda) = T_\lambda. \quad (9)$$

Here

$$\begin{aligned}
 \mathcal{M}_\lambda(\lambda) &= \mathfrak{R}^{-T}(\lambda)\mathfrak{M}\mathfrak{R}^{-1}(\lambda), \\
 C_\lambda(\dot{\lambda}, \lambda) &= \mathfrak{R}^{-T}(\lambda) \left[C(v) - \dot{\mathfrak{R}}(\lambda)\mathfrak{M}\mathfrak{R}^{-1}(\lambda) \right] \mathfrak{R}^{-1}(\lambda), \\
 D(\dot{\lambda}, \lambda) &= \mathfrak{R}^{-T}(\lambda)D(v)\mathfrak{R}^{-1}(\lambda), \\
 \mathfrak{g}_\lambda(\lambda) &= \mathfrak{R}^{-T}(\lambda)\mathfrak{g}(\lambda) \quad \text{and} \\
 T_\lambda &= \mathfrak{R}^{-T}(\lambda)\tau.
 \end{aligned} \tag{10}$$

Here

$$\mathfrak{R}(\lambda) = \begin{bmatrix} \mathfrak{R}_1(\lambda_2) & 0 \\ 0 & \mathfrak{R}_2(\lambda_2) \end{bmatrix}, \tag{11}$$

where, the $\mathfrak{R}_1(\lambda_2)$ and $\mathfrak{R}_2(\lambda_2)$ are the transformation matrices for linear and angular velocities respectively. $\mathfrak{R}_1(\lambda_2)$ and $\mathfrak{R}_2(\lambda_2)$ are defined as follows:

$$\mathfrak{R}_1(\lambda_2) = \begin{bmatrix} c\Psi & -s\Psi & 0 \\ s\Psi & c\Psi & 0 \\ 0 & 0 & 1 \end{bmatrix}, \tag{12}$$

$$\mathfrak{R}_2(\lambda_2) = \begin{bmatrix} 1 & 0 & 0 \\ 0 & 1 & 0 \\ 0 & 0 & 1 \end{bmatrix} \tag{13}$$

Here the representations c and s denote the functions $\cos(\cdot)$ and $\sin(\cdot)$ respectively.

Assumptions

- Perfect alignment is assumed between centers of gravity (O_G) and buoyancy (O_B), thus AUVs maintain horizontal stability during motion.
- The AUVs body centers are aligned with centers of gravity (O_G), thus the distance vector is $r_g = [0, 0, 0]^T$.

Remark 1 Here the motion of the AUV without any control force is assumed to be stable when it is not influenced by any control forces or torques. To establish our claim Lyapunov candidate functions is chosen to represent the summation of potential and kinetic energy as follows:

$$\mathbb{V}_1(\dot{\lambda}, \lambda) = \frac{1}{2}\dot{\lambda}^T \mathcal{M}_\lambda(\lambda)\dot{\lambda} + \int_0^\lambda \mathfrak{g}_\lambda^T(\tau) d\tau. \tag{14}$$

Now considering the time derivative of (14), we can get

$$\begin{aligned}\dot{\mathbb{V}}_1(\dot{\lambda}, \lambda) &= \frac{1}{2} \dot{\lambda}^T \dot{\mathcal{M}}_\lambda(\lambda) \dot{\lambda} + \dot{\lambda}^T \mathcal{M}_\lambda(\lambda) \ddot{\lambda} + \dot{\lambda}^T \mathfrak{g}_\lambda(\lambda) \\ &= \frac{1}{2} \dot{\lambda}^T \dot{\mathcal{M}}_\lambda(\lambda) \dot{\lambda} + \dot{\lambda}^T [\mathcal{M}_\lambda(\lambda) \ddot{\lambda} + \mathfrak{g}_\lambda(\lambda)].\end{aligned}\quad (15)$$

As $\mathcal{M}_\lambda(\lambda) = \mathcal{M}_\lambda^T(\lambda) > 0$, we can get

$$\begin{aligned}\dot{\mathbb{V}}_1(\dot{\lambda}, \lambda) &= \frac{1}{2} \dot{\lambda}^T [\dot{\mathcal{M}}_\lambda(\lambda) - 2C_\lambda(\dot{\lambda}, \lambda)] \dot{\lambda} \\ &\quad + \dot{\lambda}^T [\mathcal{M}_\lambda(\lambda) \ddot{\lambda} + C_\lambda(\dot{\lambda}, \lambda) \dot{\lambda} + \mathfrak{g}_\lambda(\lambda)].\end{aligned}\quad (16)$$

From [15] it can be verified that $\dot{\lambda}^T [\dot{\mathcal{M}}_\lambda(\lambda) - 2C_\lambda(\dot{\lambda}, \lambda)] \dot{\lambda} = 0$, thus (16) now reduced to

$$\dot{\mathbb{V}}_1(\dot{\lambda}, \lambda) = \dot{\lambda}^T [\mathcal{M}_\lambda(\lambda) \ddot{\lambda} + C_\lambda(\dot{\lambda}, \lambda) \dot{\lambda} + \mathfrak{g}_\lambda(\lambda)].\quad (17)$$

Putting $T_\lambda=0$, in (9) we obtain $[\mathcal{M}_\lambda(\lambda) \ddot{\lambda} + C_\lambda(\dot{\lambda}, \lambda) \dot{\lambda} + \mathfrak{g}_\lambda(\lambda)] = -D(\dot{\lambda}, \lambda) \dot{\lambda}$, hence

$$\dot{\mathbb{V}}_1(\dot{\lambda}, \lambda) = -\dot{\lambda}^T D(\dot{\lambda}, \lambda) \dot{\lambda}.\quad (18)$$

Thus, assuming $D(\dot{\lambda}, \lambda) > 0$ [18], we can predict the motion of AUV is stable as per Lyapunov stability theorem.

2.2. Nonlinear SMC modelling

In SMC tracking is measured by defining sliding surface \mathcal{S} as change in position as the velocity measurements are not available [3]. \mathcal{S} can be defined as

$$\mathcal{S} = \left(\overset{\sim}{\lambda}_k(\theta_k) \right) + \mathcal{G}_m \overset{\sim}{\lambda}_k(\theta_k) = \dot{\lambda}_k(\theta_k) - \dot{\lambda}_r(\theta_k),\quad (19)$$

where, $\lambda_k(\theta_k) = [x_k(\theta_k), y_k(\theta_k), \psi_k(\theta_k)]^T$ for k -th AUV, while $k = \{1, 2, \dots, N\}$. Here, N is total number of follower AUVs. \mathcal{G}_m is a diagonal matrix, which is design specific and is a positive matrix. $\overset{\sim}{\lambda}_k(\theta_k)$ depicts the errors with reference to earth fixed frame and $\dot{\lambda}_r(\theta_k)$ is the reference trajectory in the earth fixed frame. $\overset{\sim}{\lambda}_k(\theta_k)$ and $\dot{\lambda}_r(\theta_k)$ can be calculated as follows

$$\overset{\sim}{\lambda}_k(\theta_k) = \lambda_k(\theta_k) - \lambda_d.\quad (20)$$

Here λ_d is the desired position of the k -th AUV.

$$\dot{\lambda}_r(\theta_k) = \dot{\lambda}_d - \mathcal{G}_m \overset{\sim}{\lambda}_k(\theta_k).\quad (21)$$

Now we can rewrite equation (27) as

$$\ddot{\lambda}_k(\theta_k) = \dot{\mathcal{S}} + \ddot{\lambda}_r(\theta_k). \quad (22)$$

Assuming $\dot{\lambda}_r(\theta_k)$ to be smooth and bounded by λ_d , $\dot{\lambda}_d$, $\ddot{\lambda}_d$ and applying inverse velocity transformation we can obtain

$$\begin{aligned} \mathfrak{M}\dot{\mathcal{S}} = & -C(\vartheta)\mathcal{S} - D(\vartheta)\mathcal{S} \\ & + \left[\Gamma_k - \mathfrak{M}\dot{\vartheta}_r(\theta_k) - C(\vartheta)\vartheta_r(\theta_k) - D(\vartheta)\vartheta_r(\theta_k) - g(\lambda_k) \right], \end{aligned} \quad (23)$$

where $\vartheta_r(\theta_k) = \dot{\lambda}_r(\theta_k)\mathfrak{R}_1^{-1}(\varphi_k(\theta_k))$. Let $\dot{\mathcal{S}} = 0$ then we can calculate

$$\Gamma_{eqv} = \mathfrak{M}\ddot{\vartheta}_r(\theta_k) + C(\vartheta)\vartheta_r(\theta_k) + D(\vartheta)\vartheta_r(\theta_k) + g(\lambda_k) + C(\vartheta)\mathcal{S} + D(\vartheta)\mathcal{S}. \quad (24)$$

Total control input is given by

$$\Gamma = \Gamma_{eqv} + \Gamma_{sc}. \quad (25)$$

Γ_{sc} is the switching control input. For reachability to obtain in finite time with required convergence rate $s \rightarrow 0$, the dynamics of the SMC is given by

$$\dot{\mathcal{S}} = sc - \mathbb{K} \operatorname{sgn}(s), \quad (26)$$

where $c \in \operatorname{diag}(c_k)$, $\mathbb{K} \in \operatorname{diag}(\mathbb{K}_k)$, $sc_k > 0$, $\mathbb{K}_k > 0$ for $k \in (1, 2, \dots, N)$. So substituting (26) in (23) we have

$$\Gamma_{sc} = -\mathfrak{M}(sc + \mathbb{K} \operatorname{sgn}(s)), \quad (27)$$

$$\begin{aligned} \Gamma = & \mathfrak{M}\ddot{\vartheta}_r(\theta_k) + C(\vartheta)\vartheta_r(\theta_k) + D(\vartheta)\vartheta_r(\theta_k) + g(\lambda_k) \\ & + C(\vartheta)\mathcal{S} + D(\vartheta)\mathcal{S} - \mathfrak{M}(sc + \mathbb{K} \operatorname{sgn}(s)). \end{aligned} \quad (28)$$

Stability analysis of SMC

Equation (28) is the control law for nonlinear SMC. Considering the Lyapunov candidate function as

$$\dot{\mathcal{V}} = -\mathcal{S}^T c \mathcal{S} - \mathcal{S} \mathbb{K} \operatorname{sgn}(\mathcal{S}) \leq 0^T, \quad (29)$$

where c and \mathbb{K} are positive matrix to avoid anti-jamming and high frequency chattering. M is a positive matrix and is invertible. To be uniformly globally stable equation (28) must satisfy

$$\dot{\mathcal{S}}_k = -c_k \mathcal{S} - \mathbb{K}_k \operatorname{sgn}(\mathcal{S}_k), \quad \mathcal{S}_k \in \mathcal{S} \quad \text{and} \quad \mathcal{S}_k(t_0) \neq 0. \quad (30)$$

Solution of the above equation satisfying the condition $\mathcal{S}_k(t) = 0$ is

$$\mathcal{S}_k(t) = \left[|\mathcal{S}_k(t_0)| + c_k^{-1} \mathbb{K}_k \right] e^{-c_k(t-t_0)} - c_k^{-1} \mathbb{K}_k. \quad (31)$$

Sliding model will be reached at time period

$$t \geq t_0 - \ln \left[\frac{\mathbb{K}_k / (\mathbb{K}_k + c_k |\mathcal{S}_k(t_0)|)}{c_k} \right]. \quad (32)$$

3. Problem statement

Underwater environment is uncertain and hostile in nature. There are different types of underwater environments including near shore and polar ice caps. AUVs are employed in all types of marine environment to accomplish different missions such as scientific, military and commercial. GPP deals with finding a time and energy optimal or near optimal path between the source and destination points while avoiding underwater obstacles like submerged cliffs, underwater wreckages, other submersibles, sea walls and unknown sea bed changes.

3.1. Obstacle detection

The Fig. 1 the underwater environment with obstacles is represented with source and destination points. The obstacles are represented with circles of different radius. If the path of the AUV passes through any of the obstacle circles, the AUV is susceptible to collision. The AUV can avoid collision if the path is outside the radius of the circle. The path planner has to plan as a safe route by avoiding obstacle circles while minimizing time of travel and energy expenses. This path is the combination of these segments through the defined I number of waypoints. The O represents origin of the original coordinate system. The Z coordinate denotes the depth of the AUV considered to be constant.

3.2. Evaluation of path cost

Let, the starting position of AUV is given by (x_0, y_0, z_0) and the destination is at $(x_{I+1}, y_{I+1}, z_{I+1})$, where I represent the total number of internal points. Then an internal point P_i is written as (x_i, y_i, z_i) . Thus, path is represented by $OD = (x_0, y_0, z_0, \dots, x_i, y_i, z_i, \dots, x_{I+1}, y_{I+1}, z_{I+1})$. The path cost of the required path can be evaluated based on three parameters, that are “length of the path to be travelled”, “the penalty for collision”, and the “cost of diving”. Here it is assumed that there is no sudden direction change as the obstacle dimensions and positions are fixed, thus the planar trajectory is smooth. The objective is to minimize the path cost, hence minimizing all the factors contributing to path cost.

i. Path length

Total path length is the summation of the distance between the waypoints from starting point to destination. It is represented by [10],

$$L(OD) = \sum_{i=0}^I l(P_i, P_{i+1}), \quad (33)$$

where $l(P_i, P_{i+1})$ is the length of the path between the waypoints i and $i+1$.

It can be calculated as,

$$l(P_i, P_{i+1}) = \sqrt{(x_{i+1} - x_i)^2 + (y_{i+1} - y_i)^2 + (z_{i+1} - z_i)^2}. \quad (34)$$

$L(OD)$ determines total time and energy required to travel from source to destination point. Thus, it is a major contributor for the path cost.

ii. *Penalty for collision*

Penalty of collision is the extra cost encountered when the path generated for the AUV passed through the obstacle creating risk for the collision. Let, l_{\min} is the minimum safest distance that an AUV should maintain from the obstacle, r_{\min} is the minimum value of $r(P_i, P_{i+1})$ where $r(P_i, P_{i+1})$ is the smallest distance between the segment joining the points P_i and P_{i+1} and all detected static obstacles. If ρ is the positive coefficient of penalty then the risk of collision can be calculated as in [10], i.e.

$$C(OD) = \begin{cases} l_{\min} - r_{\min}, & \text{when } r_{\min} > l_{\min}, \\ e^{\rho(l_{\min} - r_{\min})} & \text{when } r_{\min} \leq l_{\min}, \end{cases} \quad (35)$$

r_{\min} can be calculated as

$$r_{\min} = \min_{i=0 \text{ to } d} r(P_i, P_{i+1}) \quad (36)$$

If $l_{\min} - r_{\min}$ is positive then the cost factor increases exponentially due to the positive ρ , which indicates increase chances of collision with obstacle.

iii. *Cost of diving*

The change in depth caused due to sudden diving of AUV leads to consumption of extra energy. Thus, cost of diving is the extra energy expends due to sudden diving of AUV, and it depends on the diving angle $\lambda(P_i, P_{i+1})$ when AUV moves from the waypoint i to $i+1$ as shown in Fig. 3. The cost of diving can be calculated as

$$G(OD) = \max_{i=0 \text{ to } d} \lambda(P_i, P_{i+1}). \quad (37)$$

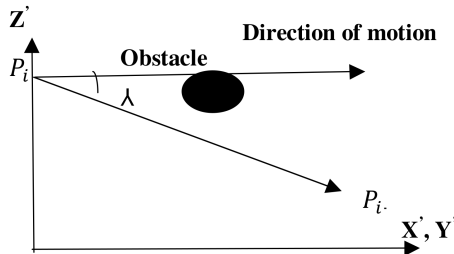


Figure 3: Angle of diving [10]

iv. *Cumulative path cost*

The cumulative path cost is the summation of all the three factors, that are $L(OD)$, $C(OD)$ and $G(OD)$. Hence the total path cost is calculated as,

$$PC(OD) = \mu L(OD) + (1 - \mu)C(OD) + G(OD), \quad (38)$$

where $\mu \in [0, 1]$, when $r_{\min} > l_{\min}$, $\mu = 1$ otherwise $\mu = 0$.

This path is subjected to the constraints as follows

$$\begin{aligned} x_{\min} < x_i < x_{\max}, & \quad \text{for } i = 0 \text{ to } I, \\ y_{\min} < y_i < y_{\max}, & \quad \text{for } i = 0 \text{ to } I, \\ 0 < z_i < z_{\max}, & \quad \text{for } i = 0 \text{ to } I. \end{aligned} \quad (39)$$

4. Communication consensus

For formation between AUVs, let a mild communication exists in underwater environment. A team of N AUVs following a leader can be represented as an undirected graph as $G_h = \{S_v, S_E, S_A\}$. Here $S_v = \{1, 2, \dots, N\} \rightarrow$ the set of nodes, $S_E \subseteq N \times N \rightarrow$ the set of edges, and $S_A = [S_{E_{kl}}] \in R^{N \times N}$ is the adjacency matrix. As per the assumption the leader may be connected or may not be connected to any of the follower AUV. The leader is tracked by the follower AUVs without velocity measurements [21]. The synchronization error $e_\theta = |\theta_k - \theta_l|$ is calculated as the difference between the position of two k -th and l -th AUVs, such that all followers move in synchronization with the leader on the basis of their local measurements when velocity measurement is not available.

The potential function (α_{kl}) is differentiable nonnegative function of $|\theta_k - \theta_l|^{-1}$, which satisfies

- i. $\alpha_{kl} = \alpha_{kl \min}$ for $\|\theta_k - \theta_l\| = d_{kl}$ where d_{kl} is required distance;
- ii. $\alpha_{kl} \rightarrow \infty$ for $\|\theta_k - \theta_l\| \rightarrow 0$;
- iii.
$$\begin{cases} \left(\frac{\partial \alpha_{kl}}{\partial \|\theta_k - \theta_l\|} \right) = 0 & \text{for } \|\theta_k - \theta_l\| \geq H, \forall k \text{ and } l \in (1, 2, \dots, N) \\ \alpha_{kl} \rightarrow \infty & \text{for } \|\theta_k - \theta_l\| \rightarrow H \text{ when } \|\theta_k - \theta_l\| < H, \\ & \forall k \text{ and } l \in (1, 2, \dots, N), \end{cases}$$
 where, H is a positive constant given by $H > \max_{k,l} (d_{kl})$;

- iv. $\alpha_{kk} = a \forall k \in (1, 2, \dots, N)$ where a is a positive constant.

The third condition ensures the initial connectivity by assuming that leader is adjacent to at least one AUV initially when operation begins. So the distributed

consensus tracking algorithm for $\dot{\theta}_k$ may be defined as [11],

$$\dot{\theta}_k = -\beta \sum_{l \in \bar{N}_k(t)} \frac{\partial \alpha_{kl}}{\partial \theta_k} - \delta_c \operatorname{sgn} \left[\sum_{l \in \bar{N}_k(t)} \frac{\partial \alpha_{kl}}{\partial \theta_k} \right] \quad (40)$$

by assuming that $l \in \bar{N}_k(t)$, $k = 1, 2, \dots, N$, $l = 0, 1, 2, \dots, N$ at time $\bar{N}_l(t) = \{1, 2, \dots\}$ denotes the neighbour set of follower k in the team consisting of the N followers and the virtual leader. The $\operatorname{sgn}[\cdot]$ represents the Signum function. The obtained path is globally optimal when $PC(OD)$ is minimum.

5. Review of GWO and its application to GPP of AUVs

5.1. Social behavior of the grey wolves

Grey wolves belong to “Canidae” species. They live in a “pack”. “Pack” is a group consisting of 12 to 15 wolves. A strict leadership hierarchy prevails in a pack as shown in Fig. 4. Alpha (A_1) wolves are the leader wolves. There is generally one male and one female A_1 wolf. They are authorized to decide the resting places, schedule the hunting etc. and are best in regulating the group. The Betas (B_t) come are next in order to the A_1 wolves. They help in decision making and maintain discipline within the pack. A ‘ B_t ’ wolf is promoted to become A_1 when an alpha wolf retires or dies. The next rank is delta (D_1). Deltas act as sentinels and generally are retired alphas and betas. They obey the orders of the dominant groups but dominate the lowest level wolves known as Omega (O_m). Omegas are the servants or the followers of other three groups [12].

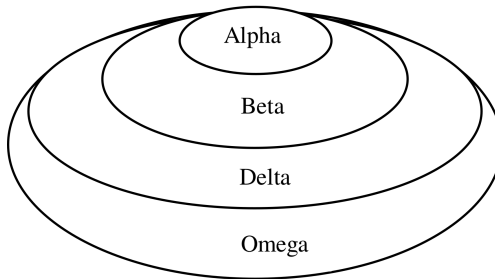


Figure 4: Grey wolf leadership hirarchy

In Fig. 4 the circle size shows the leadership hierarchy and the proportions of A_1 , B_t , D_1 and O_m wolves in a grey wolf pack. Grey wolves are pack hunter. The hunting stages are as follows [11]:

- Stage I: Approaching the targeted prey by tracing and chasing continuously.
- Stage II: Encircling and harassing the prey till it stop moving.
- Stage III: Capturing the targeted prey.

5.2. Mathematical modelling

A mathematical model has been proposed by Mirzali et.al to represent the leadership hierarchy and hunting process followed by grey wolves. The proposed model is called GWO [12]. In GWO, the first three best possible solutions in a solution space are taken as A_1 , B_t and D_1 wolves respectively. The rest of the solutions represent the O_m wolves. A_1 wolf leads the pack during hunting followed by other wolves as per their order. In initial stages of hunting they approach the target by continuously chasing it till the target gets completely encircled. These steps are modelled as shown from equation (41) to (44).

$$S(t + 1) = S_p(t) - K \cdot L. \quad (41)$$

Here, S , S_p , and t represent the current location, the targeted prey location, the number of iterations respectively. The distance vector L is defined as

$$L = |J \cdot S_p(t) - S(t)|. \quad (42)$$

The coefficient vectors are represented by K and J as given in equations (41) and (42) respectively.

$$K = 2 \cdot \gamma \cdot p_1 - \gamma, \quad (43)$$

$$J = 2 \cdot p_2. \quad (44)$$

γ is a variable that linearly decrease with each iteration t from 2 to 0. It is modelled as below,

$$\gamma = 2 - t(2/N_{iter}). \quad (45)$$

Here, N_{iter} is the total number of iterations. p_1 and p_2 are two random vectors. They can assume any value between 0 and 1 as per the location of the grey wolf. The A_1 , B_t and D_1 solutions represent better target position approximations. For t -th iteration, the three best solutions are defined as below:

$$S_1 = |S_A - K_1 \cdot L_A|, \quad (46)$$

$$S_2 = |S_B - K_2 \cdot L_B|, \quad (47)$$

$$S_3 = |S_D - K_3 \cdot L_D|. \quad (48)$$

The K_1 , K_2 and K_3 are calculated as in (43). The respective distance vectors of A_1 , B_t and D_1 are calculated as below:

$$L_A = |J_1 \cdot S_A - S|, \quad (49)$$

$$L_B = |J_2 \cdot S_B - S|, \quad (50)$$

$$L_D = |J_3 \cdot S_D - S|. \quad (51)$$

The position updating of O_m wolves is done as calculated in following equation (52)

$$S(t + 1) = (S_1 + S_2 + S_3) / 3. \quad (52)$$

5.3. GWO for GPP of multiple AUVs in formation

The algorithm for finding the optimal path for multiple AUVs in formation in the case of mild communication applying GWO is shown as a flow chart in Fig. 5.

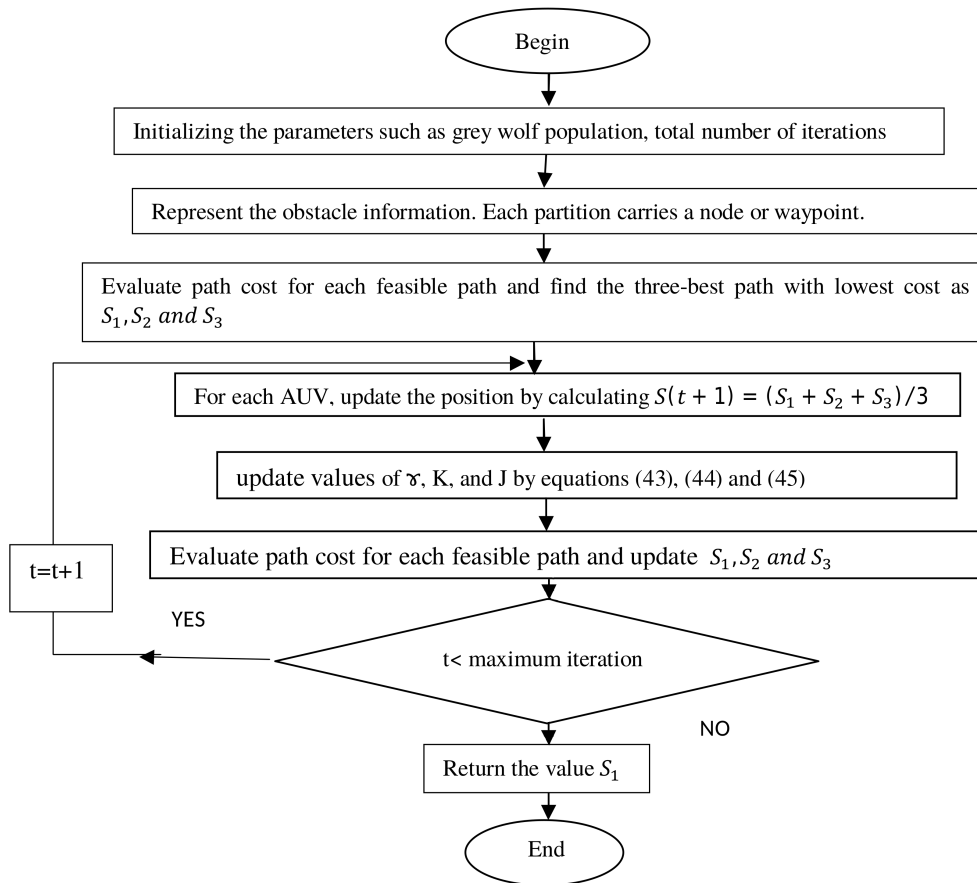


Figure 5: The flow diagram

6. Results analysis

All the algorithms are simulated using MATLAB R 2016. Simulation results are analysed in two steps:

- Step1: Global path planning.
- Step 2: Formation control of multiple AUVs using GWO.

6.1. Global path planning

GA is an effective local search technique that can solve multi-objective optimization problem. GA concept is easy to understand and can be implemented easily. It is also robust to local maxima and minima. Thus, it is preferred to solve multitude of problems related to science, engineering and commerce. Along with the advantages GA also comes with some drawbacks, that are objective function modelling and genetic operators representation in GA are very complex, it requires longer processing time that increases the computational cost. To verify that GWO inherits all the benefit of GA and requires less computational cost, both GA and GWO algorithms are applied for finding global optimal path for an AUV in a 3D environment. The source is represented by an ellipse with coordinates [50, 100, 150] and goal is represented by a rectangle with coordinates [300, 250, 350].

Three cases of obstacle environments with static obstacles are considered, that are:

- Case 1: No obstacle environment
- Case 2: Moderate obstacle environment
- Case 3: Obstacle rich environment

Case 1: No obstacle environment

Here it is assumed that AUV is moving in a clear path without any obstacle. Thus, the path between the “source point” and the “goal point” is a straight line. Figures 6a and 6b show the optimal paths obtained in this scenario by employing GA and GWO algorithms respectively. For GA the processing time is ≈ 5 second. The approximate path length and path costs are 679 and 340 units respectively.

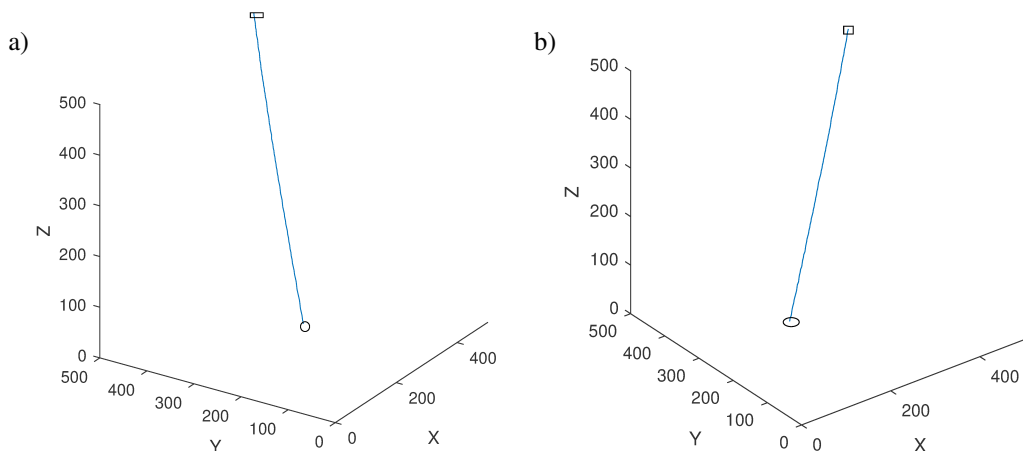


Figure 6: Path obtained in no obstacle environment: a) applying GA, b) applying GWO

In case of GWO as shown in, the processing time is ≈ 2 second. The approximate path length and path costs are 357 and 178 units respectively. Figure 7a shows the plot between fitness function versus number of generations for GA. Higher the number of generation higher is fitness. That means that optimization of cost and path increase with increased number of generations. Figure 7b shows the plot between best cost versus number of iterations for GWO. The best cost path is optimized with increase in number of iterations.

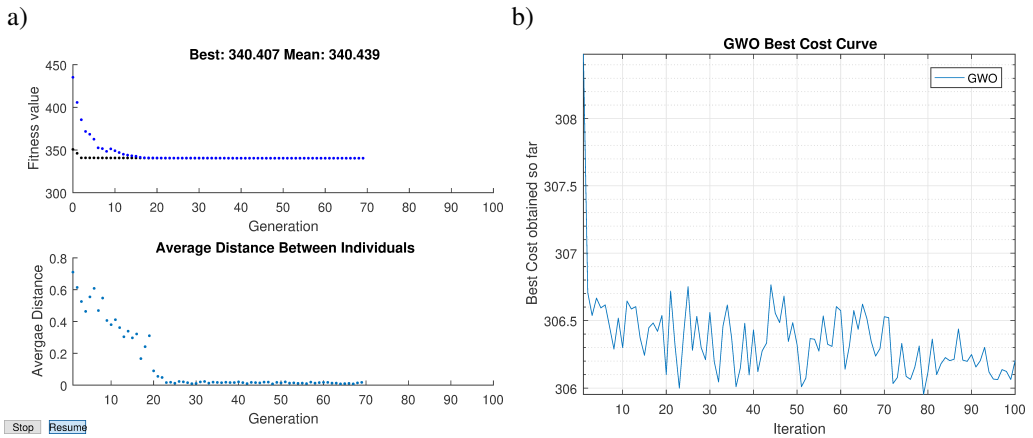


Figure 7: Comparison of GA and GWO in no obstacle environment: a) best fitness obtained in GA, b) best cost obtained in GWO

Case 2: Moderate obstacle environment

If the number of obstacles encountered during the traversal from “source point” to “goal point” is less than a predefined value N_o , then the environment is considered as moderate obstacle environment. For this experimentation $N_o \leq 5$. In this case, AUV can easily avoid the obstacles and an optimal path can be obtained.

Figures 8a and 8b show the optimal paths obtained in this case by using GA and GWO algorithms respectively. In case of GA the processing time is ≈ 7 second. The approximate path length and path costs are 983 and -1598 units respectively. In case of GWO as shown in, the processing time is ≈ 5 second. The approximate path length and path costs are 913 and -4754 units respectively. The path cost in GWO is improved by approximately 3156 units than GA. Positive path cost indicates existence of path far away from the obstacle whereas negative path cost indicates existence of path at close proximity of obstacle without colliding with it. Closer is the path lesser is the path cost. The plot between fitness function versus number of generations for GA in Fig. 9a shows improvement in cost with increased number of generations, whereas Fig. 9b shows optimization of cost with increase in number of iterations.

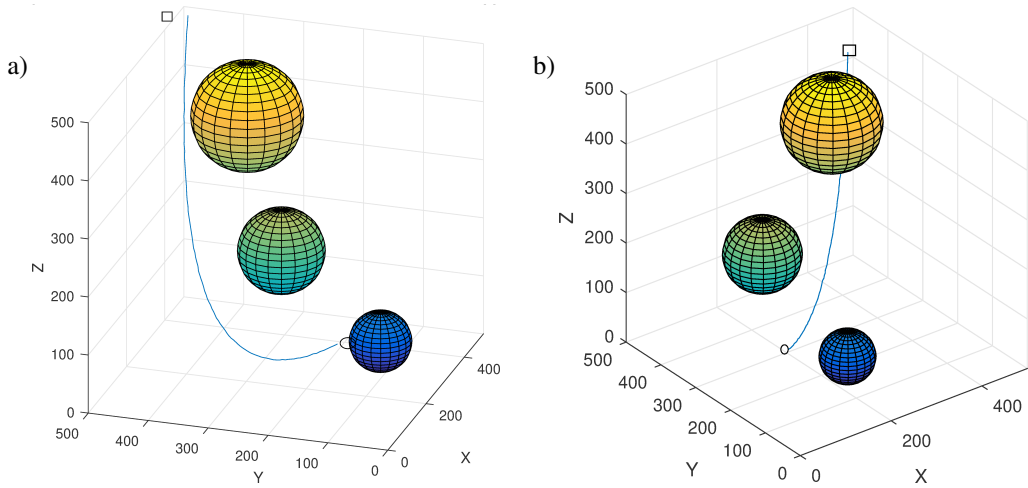


Figure 8: Path obtained in moderate obstacle environment: a) applying GA, b) applying GWO

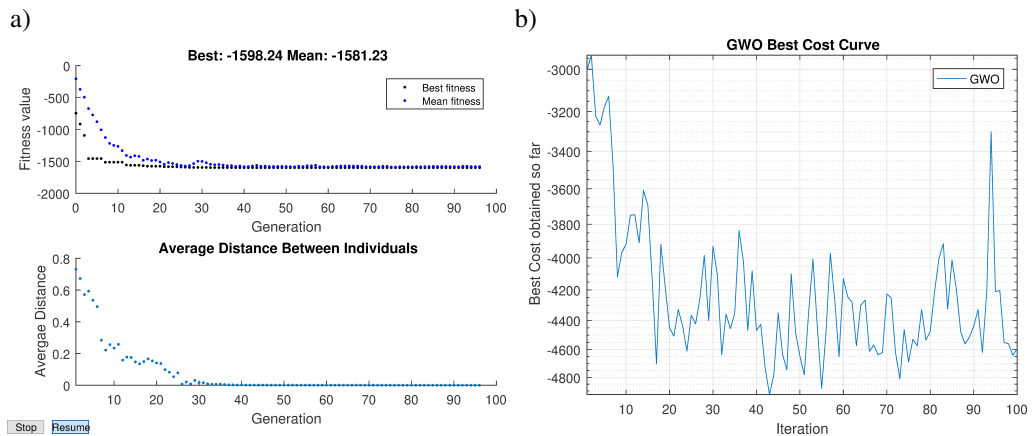


Figure 9: Comparison of GA and GWO in moderate obstacle environment: a) best fitness obtained in GA, b) best cost obtained in GWO

Case 3: Obstacle rich environment

In an obstacle rich environment number of obstacles are more than №. It is may possible that the “goal point” itself is surrounded by the obstacles. In this scenario, the AUV may has to traverse longer path to avoid obstacles and takes more time to reach the “goal point”. The computation time depends on the complexity of the environment. More the number of obstacles more is the complexities in obtaining optimal path. The increased path length and computational time lead to increase in the path cost. Figures 10a and 10b represent the optimal paths obtained in this

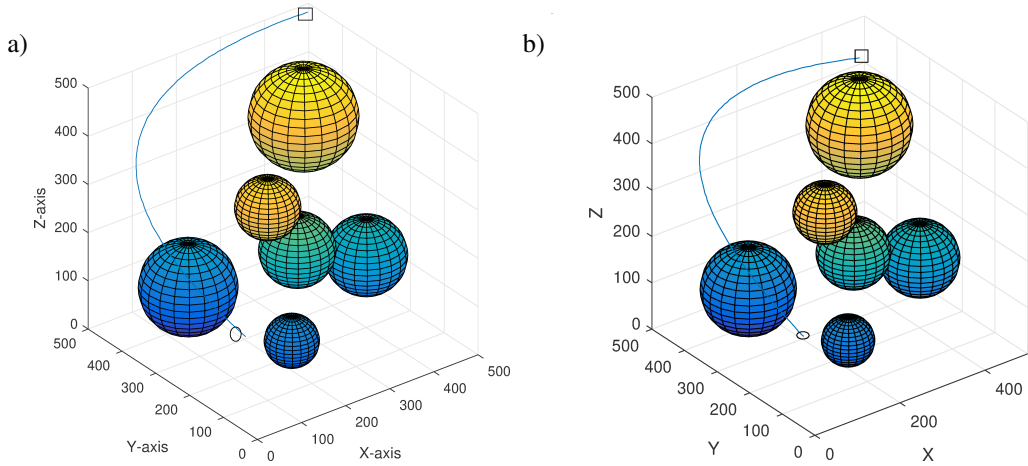


Figure 10: Path obtained in obstacle rich environment: a) applying GA, b) applying GWO

environment by employing GA and GWO algorithms respectively. The processing time is ≈ 7 seconds for both GA and GWO, but GWO is a little faster. The approximate path length for GA and GWO are 856 and 802 respectively. The path costs in case of GWO shows an improvement of 2417 units over the path cost of GA. Figure 11a shows the plot between fitness function versus number of generations for GA. Higher the number of generation higher is the fitness value resulting minimum cost path. Figure 11b shows the plot between best cost versus number of iterations for GWO. Again, the cost decrease with the increase in number of iterations.

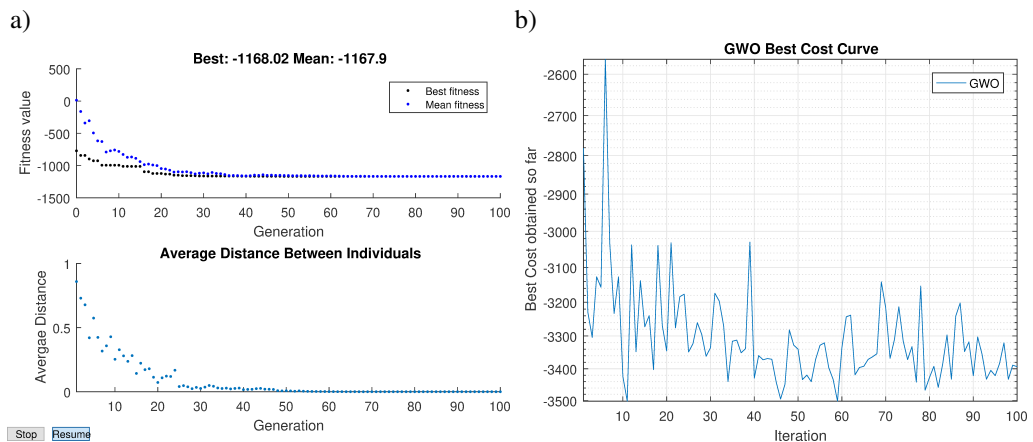


Figure 11: Comparison of GA and GWO in obstacle rich environment: a) best fitness obtained in GA, b) best cost obtained in GWO

Table 1: Performance analysis of GA and GWO

	PERFORMANCE CRITERIA	PROCESSING TIME (SEC)	PATH LENGTH	PATH COST
No obstacle environment	GA	4.622250e+00	6.792387e+02	3.405812e+02
	GWO	2.250550e+00	3.572106e+02	1.786053e+02
Moderate obstacle environment	GA	6.702076e+00	9.830163e+02	-1.598237e+03
	GWO	5.140616e+00	9.138950e+02	-4.754057e+03
Obstacle rich environment	GA	7.386708e+00	8.556970e+02	-1.168429e+03
	GWO	7.174185e+00	8.017171e+02	-3.585289e+03

6.2. Formation control of multiple AUVs using GWO

As GWO provides better cost optimized paths as compared to GA, it is employed for providing optimal paths for multiple AUVs in formation. For this experiment, the formation consists of three AUVs following leader follower configuration. It consists of one leader AUV designated as “Leader” and two follower AUVs. Follower AUVs are represented as “Follower 1” and “Follower 2”. Here two cases of formation are verified:

Case 1: When all the AUVs start from the same “Source point”.

Case 2: When AUVs start from different “Source points”.

Figure 12 and Fig. 13 show both the cases of formation for moderate obstacle and obstacle rich environment respectively. In Fig. 12a, Fig. 13a and all the AUVs

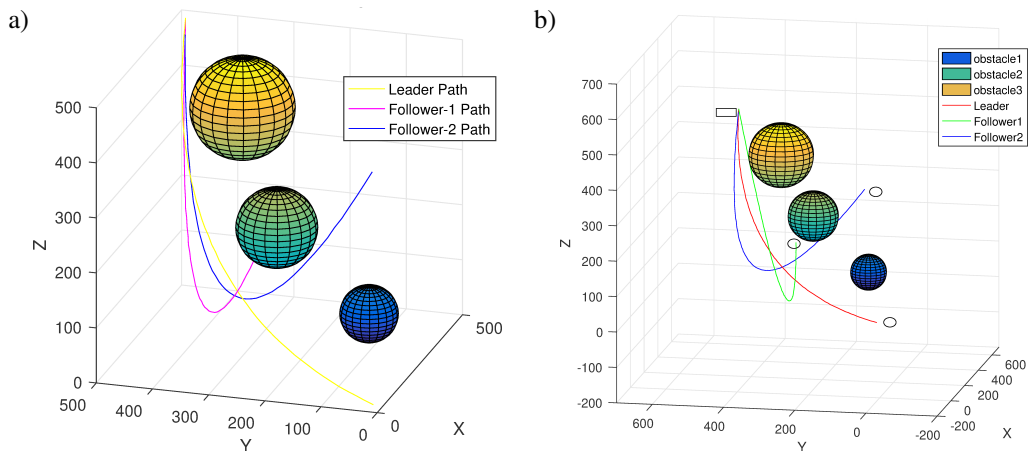


Figure 12: Formation control using GWO in moderate obstacle environment: a) with same source point, b) with different source points

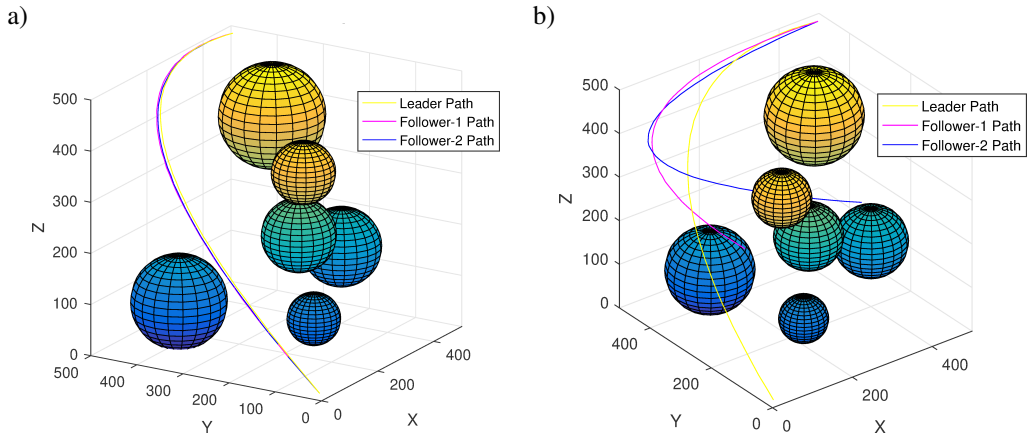


Figure 13: Formation control using GWO in obstacle rich environment: a) with same source point, b) with different source points

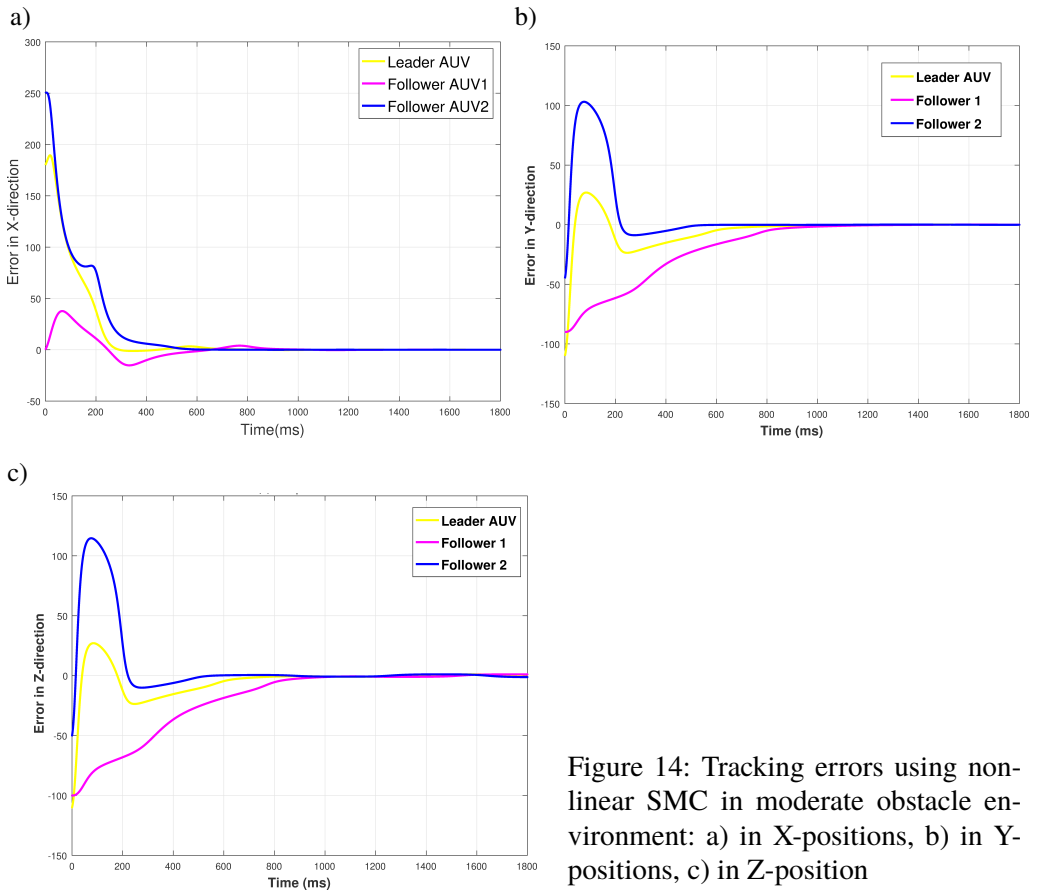


Figure 14: Tracking errors using non-linear SMC in moderate obstacle environment: a) in X-positions, b) in Y-positions, c) in Z-position

start from the same “Source point”. The “Source point” is located at coordinates $[10, 10, 10]$ and “Goal point” is with coordinates $[490, 490, 490]$. Figure 12b and Fig. 13b represent the case when AUVs start from different “Source points”. The coordinates of the “Source points” for the Leader, Follower 1 and Follower 2 are $[10, 10, 10]$, $[130, 260, 200]$ and $[300, 100, 320]$ respectively. The “Goal point” is given by the coordinates $[490, 490, 490]$. Figure 14 and 15 show the time taken for nullify the tracking error in X, Y, and Z positions for moderate obstacle and obstacle rich cases respectively. In both the figures the leader and follower AUVs trace the required path by using the proposed nonlinear SMC. Figure 16 depicts Euler angle variation for the desired paths. The AUV hydrodynamic parameters used for the simulation is given in Table 2 [3].

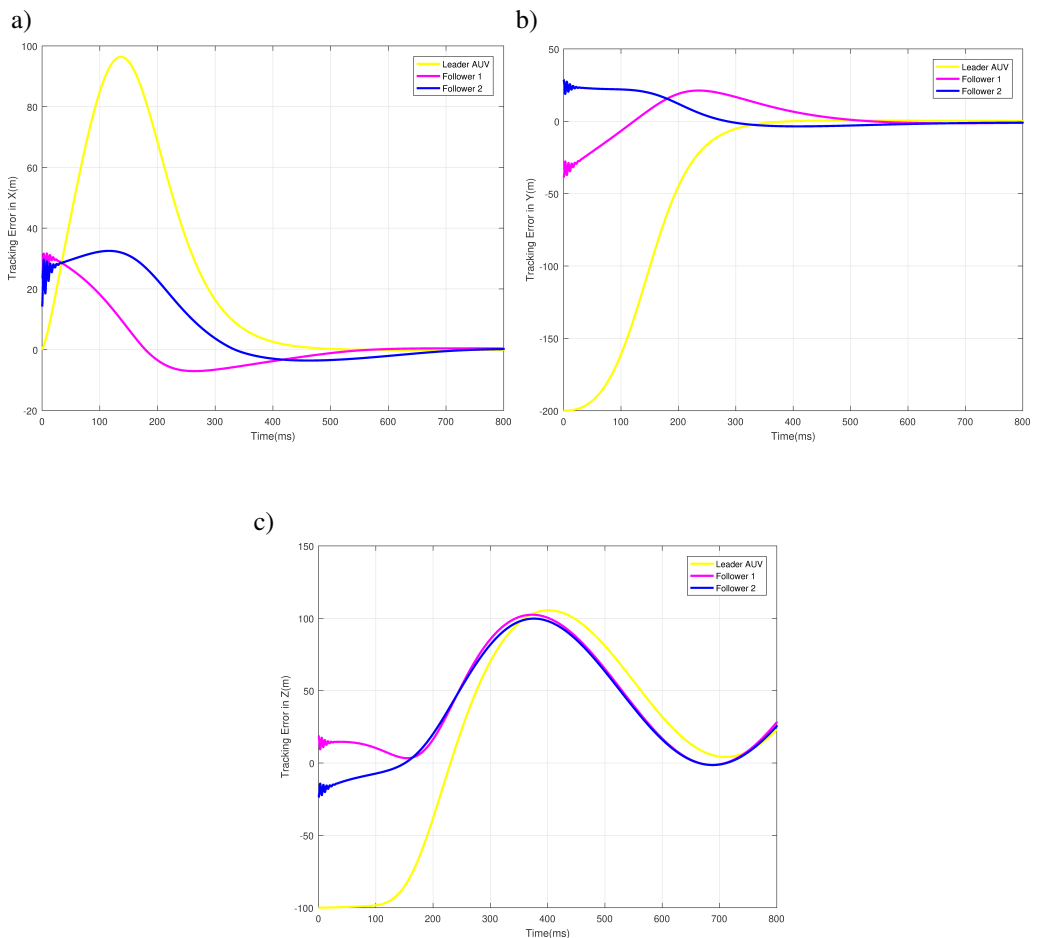


Figure 15: Tracking errors using non-linear SMC with different source point in obstacle rich environment: a) in X-positions, b) in Y-positions, c) in Z-positions

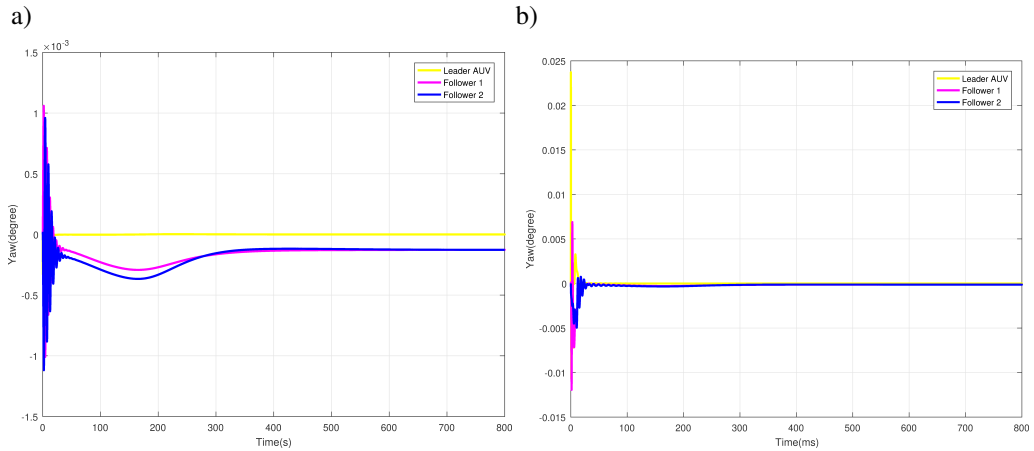


Figure 16: Yaw control using nonlinear SMC with different source points: a) in moderate obstacle environment, b) in obstacle rich environment

Table 2: AUV hydrodynamic parameters [3]

Parameters	Values	Parameters	Values
Mass	2234.5 kg	Length	4.215 m
$X_{\dot{u}}$	-141.9 kg	X_{uu}	-35.4 kg/m
$Y_{\dot{v}}$	-1715.4 kg	Y_{vv}	-667.5 kg/m
$N_{\dot{r}}$	-1349 kg·m ² /rad	N_{rr}	-310
N_{vv}	433.8 kg	X_{vr}	1715.4 kg/rad
Y_{ur}	103.4 kg/rad	N_{ur}	-1427 kg.m/rad
Y_{uv}	-346.76 kg/m	N_{vr}	-686.08 kg

7. Conclusion

GWO is a recent metaheuristic algorithm employed for various applications as evident from discussed literature. The algorithm is preferred for its remarkable exploration capability and effective local optima avoidance. It provides better approximation of the weighted path cost. But the available researches lacks in exploring GPP problem of AUV applying GWO. In this research work an attempt has been made to apply GWO for finding global optimal path for AUV. The optimal paths obtained are compared with optimal paths obtained by using GA for the GPP problem. It has been verified that GWO results in minimum cost time optimal paths as compared to GA. Thus, further GWO has been employed for finding optimal paths for multiple AUVs in “Leader-Follower” formation. The underwater environment is designed as a 3D domain with known threats. All the simulations

are done using MATLAB 2016 R. In future, this work can be extended to obtain optimal path for multiple AUVs in formation in 3D underwater environment with dynamic obstacles. Also, new hybrid algorithms can be formulated by combining features of some other well-known metaheuristic algorithm with GWO. With proper GPP, the path cost can be minimized as AUVs can reach their target in less time with less energy expenses. Thus, lower path cost leads to less expensive underwater missions.

References

- [1] B. DAS, B. SUBUDHI, and B.B. PATI: Co-operative control of a team of autonomous underwater vehicles in an obstacle-rich environment, *Journal of Marine Engineering & Technology*, **15**(1) (2016), 135–151.
- [2] X. KANG, H. XU, and X. FENG: Fuzzy logic based behavior fusion for multi-AUV formation keeping in uncertain ocean environment, *OCEANS 2009*, (2009), 1–7.
- [3] B. DAS, B. SUBUDHI, and B.B. PATI: Adaptive sliding mode formation control of multiple underwater robots, *Archives of control Sciences*, **24**(4) (2014), 515–543.
- [4] B. DAS, B. SUBUDHI, and B.B. PATI: Employing nonlinear observer for formation control of AUVs under communication constraints, *International Journal of Intelligent Unmanned Systems*, **3**(2/3) (2015), 122–155.
- [5] K. SHOJAEI: Neural network formation control of underactuated autonomous underwater vehicles with saturating actuators, *Neurocomputing*, **194** (2016), 372–384.
- [6] B. DAS, B. SUBUDHI, and B.B. PATI: Cooperative formation control of autonomous underwater vehicles: An overview, *International Journal of Automation and computing*, **13**(1) (2016), 199–225.
- [7] H. CAO, N.E. BRENER, and S. SITHARAMA IYENGAR: 3D large grid route planner for the autonomous underwater vehicles, *International Journal of Intelligent Computing and Cybernetics*, **2**(1) (2009), 455–476.
- [8] M.P. AGHABABA, M.H. AMROLLAHI, and M. BORJKHANI: Application of GA, PSO, and ACO algorithms to path planning of autonomous underwater vehicles, *Journal of Marine Science and Application*, **11**(1) (2012), 78–386.
- [9] M.P. AGHABABA: 3D path planning for underwater vehicles using five evolutionary optimization algorithms avoiding static and energetic obstacles, *Applied Ocean Research*, **38** (2012), 48–62.

- [10] M. ATAEI and A. YOUSEFI-KOMA: Three-dimensional optimal path planning for waypoint guidance of an autonomous underwater vehicle, *Robotics and Autonomous Systems*, **67** (2015), 23–32.
- [11] C. MURO, R. ESCOBEDO, L. SPECTOR, and R.P. COPPINGER: Wolf-pack (*Canis lupus*) hunting strategies emerge from simple rules in computational simulations, *Behavioural processes*, **88**(1) (2011), 192–197.
- [12] S. MIRJALILI, S.M. MIRJALILI, and A. LEWIS: Grey wolf optimizer, *Advances in Engineering Software*, **69** (2014), 46–61.
- [13] M. PANDA and B. DAS: Grey Wolf Optimizer and Its Applications: A Survey, *Proc. of the Third International Conference on Microelectronics, Computing and Communication Systems*, (2019), 179–194.
- [14] M. RADMANESH and M. KUMAR: Grey wolf optimization based sense and avoid algorithm for UAV path planning in uncertain environment using a Bayesian framework, *2016 International Conference on Unmanned Aircraft Systems (ICUAS)*, (2016), 68–76.
- [15] P. YAO and H.L. WANG: Three-dimensional path planning for UAV based on improved interfered fluid dynamical system and grey wolf optimizer, *Control and Decision*, **31**(4) (2016), 701–708.
- [16] S. ZHANG, Y. ZHOU, Z. LI, and W. PAN: Grey wolf optimizer for unmanned combat aerial vehicle path planning, *Advances in Engineering Software*, **99** (2016), 121–136.
- [17] M. PANDA, B. DAS, and B.B. PATI: Grey wolf optimization for global path planning of autonomous underwater vehicle, *Proc. of the Third International Conference on Advanced Informatics for Computing Research*, (2019), 1–6.
- [18] M. PANDA, B. DAS, B. SUBUDHI, and B.B. PATI: A Comprehensive Review of Path Planning Algorithms for Autonomous Underwater Vehicles, *International Journal of Automation and Computing*, (2020), 1–32.
- [19] B. DAS, B. SUBUDHI, and B.B. PATI: Co-operative control coordination of a team of underwater vehicles with communication constraints, *Transactions of the Institute of Measurement and Control*, **38**(4) (2016), 463–481.
- [20] T.I. FOSSEN: Guidance and Control of Ocean Vehicles, *British Library*, 6–54, 1994.
- [21] Y. CAO and W. REN: Distributed Coordinated Tracking With Reduced Interaction via a Variable Structure Approach, *IEEE Trans. Automat. Contr.*, **57**(1) (2012), 33–48.